Novel Hesperidin-Loaded Silver Nanoparticles for Targeted Cancer Drug Delivery

Sneha Salian [1], Anoop Narayanan V [1*]

Abstract

Background: Silver nanoparticles (SNPs) are increasingly recognized for their chemical stability, biocompatibility, antimicrobial properties, and intrinsic therapeutic activity. Hesperidin, a secondary metabolite found primarily in citrus fruits, is known for its potent antioxidant and anticancer properties. Loading hesperidin onto the surface of silver nanoparticles may enhance its biological activity by improving cellular penetration and enabling targeted delivery. This study aimed to formulate hesperidin-loaded silver nanoparticles and evaluate their anticancer potential. Methods: Hesperidin-loaded silver nanoparticles were formulated by reacting 1 mg of hesperidin dissolved in 10 mL of methanol with 90 mL of 1 mM silver nitrate solution, adjusted to a pH of 10. The formation of nanoparticles was confirmed by a peak at 419 nm in the UV-Visible spectra. Plain silver nanoparticles were also synthesized for comparison using trisodium citrate as a reducing agent. The formulations were characterized using Fourier Transform Infrared Spectroscopy (FTIR) to confirm the loading of hesperidin on the metal surface through the identification of corresponding functional groups. Particle size and zeta potential were measured to assess the stability and size distribution of the nanoparticles. Additionally, antioxidant activity was evaluated, and an anticancer study was performed on lung cancer cell lines to compare the cytotoxic effects of hesperidin and hesperidin-loaded silver nanoparticles. Results: The particle size of the hesperidin-loaded silver nanoparticles was found to be 96.61 ± 2.39 nm with a polydispersity index (PDI) of 0.368 ± 0.02, and a zeta potential of -19.9 ± 0.6 mV. In comparison, plain silver nanoparticles had a particle size of 95.68 ± 17.87 nm, a PDI of 0.51 ± 0.12, and a zeta potential of -27.1 ± 1.21 mV. The antioxidant activity of the hesperidin-loaded silver nanoparticles was higher compared to plain hesperidin. However, the anticancer study revealed that hesperidin alone induced higher cytotoxicity than the hesperidin-loaded silver nanoparticles on lung cancer cell lines. Conclusion: The loading of hesperidin onto silver nanoparticles enhances its antioxidant potential, suggesting a potential for targeted delivery and therapeutic applications. Despite the reduced cytotoxicity of hesperidin-loaded silver nanoparticles compared to hesperidin alone in lung cancer cell lines, further studies are warranted to explore their potential for targeted anticancer therapies.

Keywords: Hesperidin-loaded silver nanoparticles (HLSNPs), Targeted drug delivery, Cancer therapy, Green synthesis, Anticancer properties

Significance | This study showed a Hesperidin-loaded silver nanoparticles as a novel strategy for cancer therapy, enhancing bioavailability, targeted delivery, and therapeutic efficacy.

*Correspondence. Assistant Professor, NGSM Institute of Pharmaceutical Sciences, Nitte University, Mangalore, Karnataka, India
E-mail: anoopvn84@gmail.com

Editor Muhit Rana, Ph.D., And accepted by the Editorial Board May 01, 2024 (received for review Mar 15, 2024)

Introduction

Silver nanoparticles (AgNPs) have emerged as promising vehicles for the delivery of anticancer drugs due to their unique physicochemical properties, including enhanced drug solubility, stability, and bioavailability. One of the key advantages of AgNPs

Author Affiliation.
[1] Nitte, NGSM Institute of Pharmaceutical Sciences, Department of Pharmaceutics, Mangalore, Karnataka, India – 575018

Please cite this article:
Anoop Narayanan V (2024). Novel Hesperidin-Loaded Silver Nanoparticles for Targeted Cancer Drug Delivery, Biosensors and Nanotheranostics, 3(1), 1-8, 73410

is their ability to protect encapsulated drugs from degradation, thereby prolonging their circulation time in the bloodstream and facilitating tumor accumulation via the enhanced permeability and retention (EPR) effect (Singh et al., 2016; Zhao & Chen, 2020). Moreover, AgNPs can be functionalized with specific ligands to target overexpressed receptors on cancer cells, such as folate receptors, thereby minimizing the impact on healthy tissues and enhancing the therapeutic index of delivered drugs (Liu et al., 2019; Patel & Singh, 2021). This targeted delivery approach, coupled with the potential for combination with other drug delivery systems, underscores the versatility of AgNPs in cancer therapy (Kumar & Gupta, 2018; Sharma et al., 2022).

Recent studies further emphasize the role of AgNPs in combination therapies, where they can potentiate the effects of existing chemotherapeutics and help overcome drug resistance in various cancers (Almeida et al., 2017; Gupta et al., 2019). The chemical stability and biocompatibility of AgNPs are crucial attributes that enhance their applicability in drug delivery systems, ensuring that they maintain structural integrity and therapeutic efficacy in biological environments (Zhao et al., 2021). Furthermore, AgNPs exhibit low toxicity to healthy cells while effectively targeting cancer cells, making them suitable for therapeutic use (Mohan et al., 2020). The incorporation of biocompatible materials, such as chitosan, further improves the safety profile of AgNPs, promoting their use in a variety of biomedical applications (Yadav & Kumar, 2023; Sharma et al., 2023).

Biosynthesis of silver nanoparticles using phytocompounds offers several therapeutic advantages. Utilizing green techniques enhances the biocompatibility and effectiveness of nanoparticles while minimizing pollution. Green synthesis is more cost-effective and straightforward than conventional chemistry. Plant extracts mitigate and stabilize costly, hazardous chemicals, the need for significant energy consumption, and intricate machinery (Geetha et al., 2013; Pal & Agrawal, 2022). Empirical evidence from the studies conducted by Geetha et al. (2013) and Pal & Agrawal (2022) demonstrates that the extraction of leaves from Pimenta dioica and Ocimum tenuiflorum can effectively and reliably convert silver ions into nanoparticles. Green chemistry decreases manufacturing expenses and advances sustainability.

Plant extract phytocompounds exhibit biological properties that augment the effectiveness of nanoparticle therapy. The silver nanoparticles produced from Gymnema sylvestre and Moringa oleifera extracts show promising antibacterial and antihypertensive properties (Rajesh et al., 2018; Singh et al., 2021). The extracts are enriched with natural antioxidants and phytochemicals that enhance the stability and functionality of nanoparticles, so increasing their bioavailability and medical effectiveness. Nanoparticle size and morphology can be regulated by manipulating synthesis parameters such as temperature, pH, and plant extract concentration (Ali et al., 2017). Efficient control is necessary to maximize the performance of particles in drug delivery and therapeutic applications. Precision drug delivery is essential because the size and shape of silver nanoparticles impact their cellular uptake and biological activity. Employing non-toxic botanical extracts enhances the safety of nanoparticles in biological systems. A range of plant-derived silver nanoparticles selectively attacks cancer cells with minimal harm to normal cells (Ravi et al., 2020). Selective toxicity enables cancer patients to prevent harm to healthy tissues.

Hesperidin, a flavonoid predominantly found in citrus fruits, is recognized for its potent anticancer properties, particularly in the context of lung cancer and other malignancies. Hesperidin has demonstrated significant tumor growth inhibition in non-small cell lung cancer (NSCLC) and prostate cancer through mechanisms such as apoptosis induction, modulation of signaling pathways, and inhibition of cell migration and invasion (Ghosh et al., 2018; Wang & Li, 2020). Specifically, hesperidin has been shown to inhibit lung cancer cell proliferation and trigger apoptosis by intervening in the miR-132/ZEB2 signaling pathway, which plays a crucial role in epithelial-mesenchymal transition (EMT), a process associated with cancer metastasis. Additionally, hesperidin stimulates apoptotic signaling pathways, such as cleaved caspase-3, in NSCLC cell lines (Liu et al., 2017; Zheng et al., 2021).

Beyond lung cancer, hesperidin exhibits broad-spectrum anticancer activity by inducing oxidative stress, disturbing calcium homeostasis, and modulating endoplasmic reticulum stress signaling pathways (Chen & Zhu, 2019; Patel et al., 2021). It also plays a crucial role in regulating inflammatory pathways, which is vital for decelerating tumor proliferation in renal and gastric malignancies (Patel et al., 2021; Gupta et al., 2022; Li et al., 2023). Moreover, hesperidin's ability to enhance cancer cell responsiveness to chemotherapy drugs such as cisplatin highlights its potential as a supplementary therapy (Wang et al., 2023).

The chemical stability, biocompatibility, and targeted delivery capabilities of AgNPs, combined with the potent anticancer properties of hesperidin, position hesperidin-loaded silver nanoparticles (H-SNPs) as a promising therapeutic strategy. The integration of these two entities may not only improve the bioavailability and efficacy of hesperidin but also pave the way for innovative approaches in cancer treatment.

Materials and Methods

Materials

The following chemicals and reagents were utilized in this study: Silver Nitrate ($AgNO_3$), Hesperidin, Dimethyl Sulfoxide (DMSO), and Tris (Free Base) were procured from Himedia, Mumbai, India. Trisodium Citrate was obtained from Spectrochem Pvt. Ltd., Mumbai, while Sodium Hydroxide (NaOH) was purchased from

LobaChemie, Mumbai. Methanol (CH_3OH) was sourced from Nice Chemicals, Kerala, India. Additionally, Sulforhodamine B powder and Trichloroacetic Acid (TCA) were acquired from Sigma-Aldrich. Potassium Chloride (KCl) was also utilized, with its source specified in the experiment. All chemicals were of analytical grade and were used without further purification unless otherwise stated.

Methods

Analytical method development

To determine the absorption maxima (λmax) and construct the calibration curve for hesperidin, a stock solution (1000 µg/mL) was prepared by dissolving 50 mg of hesperidin in DMSO. This was further diluted to obtain concentrations ranging from 5 to 30 µg/mL. The absorbance of these samples was measured at 287 nm using a UV-Vis spectrophotometer, and a calibration curve was constructed by plotting absorbance against concentration, with all measurements performed in triplicate.

Formulation of Hesperidin-Loaded Silver Nanoparticles (HLSNP)

Hesperidin-loaded silver nanoparticles (HLSNP) were synthesized by first dissolving silver nitrate ($AgNO_3$) in distilled water to prepare a 1 mM solution. This solution was then mixed with hesperidin dissolved in DMSO, where hesperidin acted as both the reducing and stabilizing agent. The reaction mixture was stirred at room temperature at 1500RPM in a magnetic stirrer, until a noticeable color change indicated the formation of HLSNP. The nanoparticles were subsequently purified through centrifugation, followed by washing with distilled water and drying for further analysis.

Plain silver nanoparticles were prepared using the above method, where trisodium citrate was used instead of Hesperidin.

Characterization of HLSNP

UV-visible spectrophotometer analysis

The synthesized HSNPs and SNPs were subjected to UV spectral analysis in the wavelength range of 300–800 nm. The observed color change from colorless to brown for both HSNPs and SNPs indicates the successful formation of silver nanoparticles, as confirmed by UV spectroscopy.

Determination of Average Particle Size, Particle Size Distribution, and Zeta Potential

The average particle size, zeta potential, and polydispersity index (PDI) of both hesperidin-loaded silver nanoparticles (HSNPs) and plain silver nanoparticles (SNPs) were determined using dynamic light scattering (DLS) with a Malvern Zetasizer. The samples were diluted in a suitable dispersion medium, and measurements were conducted at 25°C. Each sample was analyzed in triplicate to ensure accuracy and reproducibility. The DLS technique provided information on the particle size distribution, with the average particle size calculated from intensity distribution, PDI indicating the distribution width, and zeta potential assessing surface charge. The results were reported as the mean values with standard deviations, reflecting the true characteristics of the synthesized nanoparticles.

FT-IR Spectrometric Studies

Fourier-transform infrared spectroscopy (FTIR) was employed to predict the physicochemical interactions between various excipients in the formulations. The FTIR spectra of both the hesperidin-loaded silver nanoparticles (HSNPs) and plain silver nanoparticles (SNPs) were compared with the IR peaks of pure hesperidin and silver nitrate obtained in the preformulation study. This comparison helps to identify any shifts or changes in peak positions, which may indicate interactions between the excipients and the active components.

Drug Loading Efficiency

The drug loading efficiency of hesperidin-loaded silver nanoparticles (HSNPs) was determined using the calibration curve method. Specifically, 10 mg of HSNPs was dissolved in 1 ml of dimethyl sulfoxide (DMSO). The resulting solution was analyzed using a UV spectrophotometer (Shimadzu, model 1700, Japan) at a wavelength of 287 nm, which corresponds to the peak absorbance established in the calibration curve. This method allowed for accurate quantification of hesperidin content within the nanoparticle formulation and the assessment of its loading efficiency.

Scanning Electron Microscopy (SEM)/Energy Dispersive X-ray (EDX) Analysis of Hesperidin-Loaded Silver Nanoparticles

The formulated hesperidin-loaded silver nanoparticles were analyzed using field emission scanning electron microscopy (FESEM) to evaluate their surface morphology, texture, and particle distribution. Prior to the analysis, the sample underwent gold sputtering to enhance conductivity. The FESEM was operated at an accelerating voltage of 5.00 kV with a magnification of 180.00 KX. This analysis provided detailed insights into the structural characteristics of the nanoparticles. Additionally, energy dispersive X-ray (EDX) analysis was conducted to identify the elemental composition of the nanoparticles.

Antioxidant Study of Silver Nanoparticles

The in vitro antioxidant activity of the silver nanoparticles was evaluated using the DPPH (2,2-diphenyl-1-picrylhydrazyl) method. For this study, 2 mg of hesperidin-loaded silver nanoparticles (HSNPs) was dissolved in 1 ml of methanol to prepare a stock solution with a concentration of 2000 µg/ml. From this stock solution, aliquots of 5, 10, 20, 30, 40, and 50 µl were taken, and to each aliquot, 375 µl of DPPH solution was added. The final volume was adjusted to 2 ml using methanol. Ascorbic acid was used as the standard for comparison, while a mixture of DPPH and methanol served as the blank.

The samples were incubated in the dark for 1 hour at room temperature to allow the reaction to occur. After incubation, the

absorbance was measured at 517 nm using a UV spectrophotometer. This procedure was repeated for pure hesperidin, plain silver nanoparticles (SNPs), and ascorbic acid. All experiments were conducted in triplicate to ensure the accuracy and reproducibility of the results.

The percentage of DPPH radical scavenging activity was calculated using the following formula:

% Scavenging = (A0−A1)×100/A0

Where:

- A0 is the absorbance of the blank,
- A1is the absorbance of the sample.

This analysis provided a comparative evaluation of the antioxidant potential of HSNPs, pure hesperidin, plain SNPs, and ascorbic acid.

Anticancer Study of Silver Nanoparticles

Trypan Blue Test for Cell Viability and SRB assay

Huh-7 cells were first washed with phosphate-buffered saline (PBS) and then trypsinized by adding 2 ml of trypsin in a T25 flask. Following trypsinization, 2 ml of DMEM (Dulbecco's Modified Eagle Medium) was added to the flask, and the contents were transferred to a sterile 1.5 ml centrifuge tube using a pipette. In a separate Eppendorf tube, 20 µl of trypan blue solution was mixed with 20 µl of the cell culture. The haemocytometer was thoroughly washed and dried, and 18 µl of the trypan blue-stained cell solution was added to the first slot, with another 18 µl added to the second slot. The haemocytometer was then inserted into the cell counter to determine cell viability.

Cell Seeding

After adjusting the cell concentration, 100 µl of the cell culture was seeded into each well of a 96-well plate. The plate was incubated at 37°C in a 5% CO_2 incubator for one day to allow the cells to adhere and grow.

Cell Fixation and Staining

The cell culture supernatant was carefully removed from the 96-well plate using a pipette. The first and twelfth lanes were used as controls, with 200 µl of complete growth media added to each well in these lanes. In the wells of lanes two through six, 20 µl of hesperidin-loaded silver nanoparticles (HSNPs) were added at different concentrations (20, 40, 60, 80, and 100 µl). In the wells of lanes seven through eleven, 10 µl of plain silver nanoparticles (SNPs) were added at different concentrations (10, 20, 30, 40, and 50 µl).

After the appropriate treatments were added to each well, the cells were incubated for 24 hours at 37°C in a CO_2 incubator. Each well was then treated with 30 µl of 50% trichloroacetic acid (TCA), and the plate was incubated at 4°C for 1 hour to fix the cells. After the incubation period, the plate was washed under slow-running tap water and allowed to dry at room temperature for 12 hours. Next, 100 µl of 0.4% sulforhodamine B (SRB) reagent was added to each well, and the plate was left at room temperature for 1 hour to stain the cellular proteins. The plate was then rinsed with 1% acetic acid to remove any unbound dye. Finally, the optical density (O.D.) of the wells was measured using a spectrophotometer to assess cell viability and the anticancer activity of the nanoparticles.

Results and discussion

Analytical method development

The UV spectrum of hesperidin in dimethyl sulfoxide (DMSO) displayed a peak at 287 nm, identified as the absorption maximum (λmax) for the study. A calibration curve was then constructed by measuring the absorbance of various hesperidin concentrations in DMSO at 287 nm using a UV-Vis spectrophotometer (Simadzu, 1700, Japan). The curve demonstrated a linear relationship with a regression coefficient (R^2) of 0.999, confirming that hesperidin follows Beer's Lambert law within the concentration range of 5-30 µg/ml. This method was deemed reliable for further analysis in the study.

Formulation of silver nanoparticles

The procedure for formulating hesperidin-loaded silver nanoparticles (HSNP) and plain silver nanoparticles (SNP) is detailed in the methods section. During the reaction, the primary indicator of silver nanoparticle formation is the change in color of the reaction mixture. This color change is attributed to the excitation of surface Plasmon resonance on the metal ions, with a transition to a brown color indicating the successful formation of silver nanoparticles.

To further confirm nanoparticle formation, the Faraday-Tyndall effect was observed using a laser beam, which helps validate the presence of nanoparticles based on light scattering. Additionally, the pH of the reaction mixture plays a critical role in influencing the shape and size of the nanoparticles. pH variations affect the electrical charges on the capping agents, altering their potential to bind with and reduce metal ions, which consequently impacts the characteristics of the formed nanoparticles.

Evaluation of silver nanoparticles

UV-Visible Spectrophotometric Analysis of Formulated Silver Nanoparticles

The UV-visible spectrophotometric analysis of the formulated HSNP was conducted to exploit their distinctive optical properties. Silver nanoparticles interact with specific wavelengths of light due to the close proximity of their valence and conduction bands, which allows for the free movement of electrons. This freedom results in surface Plasmon resonance (SPR), where the collective oscillation of the free electrons in the silver nanoparticles resonates with the incoming light wave.

The confirmation of silver nanoparticle formation was achieved through UV-visible spectroscopy, which revealed a characteristic peak at 419 nm. This peak is indicative of the SPR effect, confirming

the successful synthesis of silver nanoparticles and their unique optical behavior.

Average Particle Size, Particle Size Distribution, and Zeta Potential Determination of Silver Nanoparticles

The formulated silver nanoparticles were analyzed for average particle size, polydispersity index (PDI), and zeta potential using the Malvern Zetasizer. The results, expressed as the mean of three replications ± standard deviation, are summarized in Table 1.

Dynamic Light Scattering (DLS), the principle behind the Malvern Zetasizer, is widely used to study hydrodynamic particle size and distribution. This technique measures the average particle diameter and the PDI, which indicates the width of the particle size distribution. For the hesperidin-loaded SNP, a PDI of 0.368 ± 0.02 was observed, suggesting a relatively uniform size and homogeneous distribution. In contrast, the plain SNP exhibited a higher PDI of 0.51 ± 0.12, indicating a broader size distribution.

The zeta potential, which assesses the surface charges on the particles, was also measured. The zeta potential for plain SNP was -27.1 ± 1.21 mV, while for the hesperidin-loaded SNP, it was -19.9 ± 0.6 mV. The relatively high zeta potential values in both formulations signify substantial repulsive forces between particles, which helps prevent agglomeration and enhances the stability of the nanoparticles.

FTIR spectrophotometric studies

The FTIR study was conducted to identify the functional groups present in hesperidin and silver nitrate by comparing the obtained spectra with standard values. The analysis revealed a peak at 1359.45 cm^{-1}, corresponding to the O-H group, indicating the presence of a phenolic compound in hesperidin. Additional peaks were observed at 1645.38 cm^{-1}, 1204.12 cm^{-1}, 2936.93 cm^{-1}, and 3552.79 cm^{-1}, corresponding to C-H (aromatic), C-O (alkyl aryl ether), C-H (alkane), and O-H (alcohol) groups in hesperidin, respectively. In the case of silver nitrate, the presence of a peak at 1650.89 cm^{-1} was attributed to the N-O group. These findings confirm the characteristic functional groups in both hesperidin and silver nitrate.

The FTIR analysis of hesperidin-loaded silver nanoparticles (HSNP) was performed to identify the functional groups involved in the capping and stabilization of the nanoparticles. The spectrum of HSNP showed peaks at 3556.27 cm^{-1} (O-H group, alcohol), 2923.71 cm^{-1} (C-H group, alkane), 1765.52 cm^{-1} (C-H group, aromatic), 1379.40 cm^{-1} (O-H group, phenol), and 1565.73 cm^{-1} (N-O group, nitro). In contrast, the plain silver nanoparticles (SNP) exhibited a peak at 1511.22 cm^{-1} for the N-O group.

The shift in the N-O group peak from 1565.73 cm^{-1} in HSNP to 1511.22 cm^{-1} in plain SNP suggests a change in the electronic environment of the nitro group due to interaction with hesperidin. This shift indicates that the nitro group in HSNP is involved in bonding with the silver nanoparticles, which may result from the reduction and stabilization processes during nanoparticle synthesis. The interaction between hesperidin and silver ions could alter the nitro group's electronic characteristics, leading to this observed shift. Such changes highlight the role of functional groups in stabilizing the nanoparticles and their potential involvement in the formation of the HSNP complex.

Hesperidin loading efficiency

The loading efficiency of the formulation was evaluated, and the drug loading efficiency was found to be 56%. This relatively high loading efficiency indicates that a significant amount of hesperidin was successfully encapsulated within the silver nanoparticles. High drug loading efficiency is crucial for maximizing therapeutic efficacy while minimizing the required dose, thus enhancing the overall performance of the formulation.

SEM and EDX analysis of hesperidin loaded silver nanoparticle

The SEM analysis of hesperidin-loaded silver nanoparticles (HSNP) revealed that the particles were predominantly spherical in shape and showed some degree of agglomeration (Figure 1). The particle size was found to be below 100 nm, with the agglomeration likely resulting from the drying process, which may cause particles that are otherwise stable in liquid form to clump together. EDX analysis provided further confirmation of the nanoparticles' composition. The energy dispersive X-ray (EDX) spectrum of HSNP exhibited a characteristic signal peak at 3 keV, indicative of surface plasmon resonance (SPR) typically associated with metallic silver nanoparticles. Quantitative data from the EDX spectrum revealed that the percentage weight of silver in the HSNP was 18.4%, further validating the successful synthesis and composition of the nanoparticles.

Antioxidant Activity of silver nanoparticles

The antioxidant activity of the tested materials was assessed using the DPPH free radical scavenging assay. The results, expressed as percentage scavenging activity, demonstrated a concentration-dependent increase across all materials tested. The IC50 values, which indicate the concentration required to achieve 50% scavenging activity, were also calculated and are shown in Table 2 and the comparison is also depicted in Figure 2.

Anticancer Study of HSNP in Huh-7 liver cancer Cells

The anticancer activity of hesperidin and hesperidin-loaded silver nanoparticles (HSNP) was evaluated in Huh-7 cells using the Sulforhodamine B (SRB) assay. The results demonstrated that HSNP exhibited better anticancer activity compared to hesperidin alone and plain silver nanoparticles (SNP). This enhanced activity can be attributed to the nanoscale delivery system, which improves the bioavailability and cellular uptake of hesperidin in Huh-7 cells. Hesperidin's anticancer mechanism involves inducing apoptosis, inhibiting cell proliferation, and modulating key signaling pathways essential for cancer cell survival. It has been shown to downregulate

Table 1. Average Particle Size, Polydispersity Index (PDI), and Zeta Potential of Silver Nanoparticles

Formulation	Particle Size (nm)	PDI	Zeta Potential (mV)
Hesperidin-Reduced SNP	96.61 ± 2.39	0.368 ± 0.02	-19.9 ± 0.6
Plain SNP	95.68 ± 17.87	0.51 ± 0.12	-27.1 ± 1.21

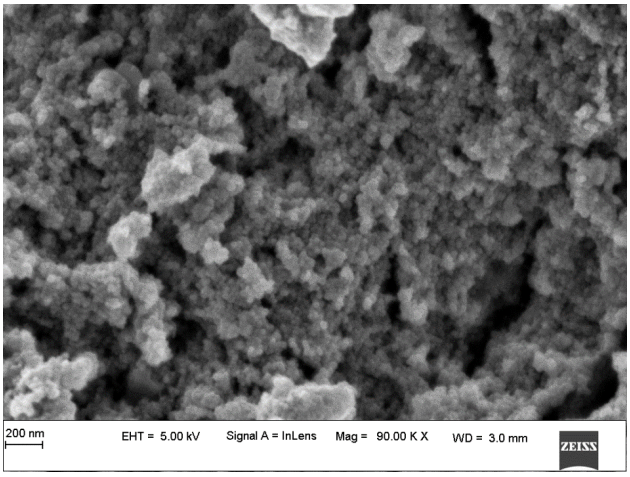

Figure 1. SEM image of HSNP showing spherical particles of uniform size.

Table 2. Antioxidant activity of formulated HSNP and SNP against Hesperidin measured by DPPH assay

	Tested material	Concentration (µg/ml)						IC 50 (µg/ml)
		5	10	20	30	40	50	
DPPH % Scavenging Activity ± S.D*	**Ascorbic Acid**	57.69 ± 4.71	56.41 ± 19.5	71.15 ± 4.15	75.00 ± 3.14	77.56 ± 2.39	79.48 ± 0.90	37.01
	HSNP	52.18 ± 2.28	54.96 ± 2.66	61.65 ± 4.09	57.1 ± 13.4	67.78 ± 0.94	68.08 ± 1.26	87.01
	SNP	37.79 ± 0.91	49.30 ± 4.69	55.06 ± 2.03	60.07 ± 0.57	62.58 ± 1.83	72.28 ± 1.31	40.61
	Hesperidin	28.59 ± 0.47	30.54 ± 0.94	36.21 ± 1.80	41.22 ± 1.49	46.42 ± 1.85	56.26 ± 0.99	60.13

*Mean of 3 replications ± SD.

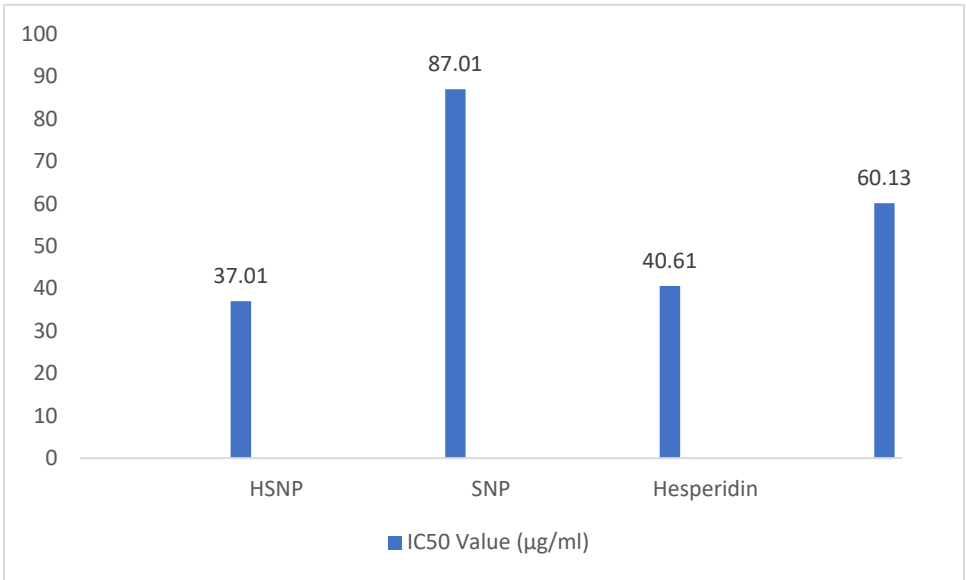

Figure 2. Comparison of IC 50 values of HSNP and SNP against Hesperidin and ascorbic acid as a reference compound

pro-survival proteins and activate caspases, leading to programmed cell death in cancer cells (Aggarwal et al., 2020). When incorporated into silver nanoparticles, hesperidin's effectiveness is enhanced due to improved cellular uptake and the enhanced permeability and retention (EPR) effect, which allows nanoparticles to accumulate more efficiently in tumor tissues (Gomes et al., 2021).

Silver nanoparticles alone also exhibit significant anticancer properties. Their mechanism involves generating reactive oxygen species (ROS), which can damage cellular components such as DNA, proteins, and lipids, leading to oxidative stress and eventual cell death. SNPs can also disrupt mitochondrial function, leading to apoptosis, and interfere with cell membrane integrity, further promoting cytotoxicity. Additionally, silver nanoparticles can modulate the expression of genes involved in cell cycle regulation and apoptosis, enhancing their anticancer potential (Dayem et al., 2017).

The combination of these mechanisms in HSNPs results in a more potent anticancer effect in Huh-7 cells compared to hesperidin or SNPs alone. The synergy between hesperidin's bioactive properties and the intrinsic cytotoxicity of silver nanoparticles makes HSNP a promising candidate for liver cancer treatment.

Yao et al. (2022) demonstrated that hesperidin inhibits lung cancer in vitro and in vivo through the PinX1 pathway, while Kong et al. (2020) showed that hesperetin, a hesperidin derivative, reverses P-glycoprotein-mediated cisplatin resistance in DDP-resistant human lung cancer cells via modulation of the nuclear factor-κB signaling pathway. Furthermore, hesperidin has been shown to downregulate pro-survival proteins and activate caspases, leading to programmed cell death in cancer cells (Aggarwal et al., 2020). When incorporated into silver nanoparticles, hesperidin's effectiveness is enhanced due to improved cellular uptake and the enhanced permeability and retention (EPR) effect, which allows nanoparticles to accumulate more efficiently in tumor tissues (Gomes et al., 2021).

Conclusion

This study successfully synthesized hesperidin-loaded silver nanoparticles (HSNP) using the bioflavonoid hesperidin as both a reducing and capping agent. The distinct surface plasmon resonance (SPR) peak observed in HSNP confirms successful nanoparticle formation, with UV and FTIR analyses further verifying the capping of hesperidin on the silver nanoparticles. HSNP demonstrated enhanced antioxidant activity and promising anticancer potential in Huh-7 cells compared to both plain hesperidin and silver nanoparticles, suggesting that nanonization may enhance the bioactivity of hesperidin. However, the study faced potential biases, including the variability in drug loading efficiency and the limitations of in vitro models, which might not fully represent in vivo conditions. These factors could influence the observed outcomes and should be considered when interpreting the results. Future research should aim to optimize drug loading to improve the therapeutic efficacy of HSNP, particularly in cancer treatment. Additionally, exploring the in vivo effects, potential clinical applications, and addressing any inherent biases in the study design could provide valuable insights into the broader use of HSNP as a multifunctional therapeutic agent.

Author contributions

S.S. and A.N.V. formulated the study objectives, constructed the hypotheses, and revised the manuscript, conducted the literature review and was responsible for data collection and analysis. The author reviewed and approved the final manuscript.

Acknowledgment

Author was grateful to their department.

Competing financial interests

The authors have no conflict of interest.

References

Banu, A., Gousuddin, M., & Yahya, E. B. (2021). Green synthesized monodispersed silver nanoparticles' characterization and their efficacy against cancer cells. Biomedical Research and Therapy, 8, 4476–4482. https://doi.org/10.15419/bmrat.v8i8.686

Bhakat, C. (2012). Effects of silver nanoparticles synthesize from Ficus benjamina on normal cells and cancer cells. IOSR Journal of Pharmacy and Biological Sciences, 1, 33–36. https://doi.org/10.9790/3008-0143336

Birsu Cincin, Z., Unlu, M., Kiran, B., Sinem Bireller, E., Baran, Y., & Cakmakoglu, B. (2015). Anti-proliferative, apoptotic and signal transduction effects of hesperidin in non-small cell lung cancer cells. Cellular Oncology (Dordrecht, Netherlands), 38, 195–204. https://doi.org/10.1007/s13402-015-0222-z

Chang, D., Ma, Y., Xu, X., Xie, J., & Ju, S. (2021). Stimuli-responsive polymeric nanoplatforms for cancer therapy. Frontiers in Bioengineering and Biotechnology, 9, 707319. https://doi.org/10.3389/fbioe.2021.707319

Faisal, S., Hamed, A. A., Shawky, R. M., & Emara, M. (2023). Chitosan-silver nanoparticles: A versatile conjugate for biotechnological advancements. Journal of Advanced Pharmacy Research, 7, 163–169. https://doi.org/10.21608/aprh.2023.218891.1222

Garcia-Bennett, A., Nees, M., & Fadeel, B. (2011). In search of the holy grail: Folate-targeted nanoparticles for cancer therapy. Biochemical Pharmacology, 81, 976–984. https://doi.org/10.1016/j.bcp.2011.01.023

Gregoriou, Y., Gregoriou, G., Manoli, A., Papageorgis, P., Mc Larney, B., Vangeli, D., McColman, S., Yilmaz, V., Hsu, H. T., Skubal, M., & et al. (2023). Photophysical and biological assessment of Coumarin-6 loaded polymeric nanoparticles as a cancer imaging agent. Sensors & Diagnostics, 2, 1277–1285. https://doi.org/10.1039/D3SD00065F

J, B. (2024). Characterization and evaluation of green synthesized silver nanoparticles using Moringa oleifera leaf extract and its antihypertensive activity. Annals of Clinical

and Medical Case Reports, 13, 01–09. https://doi.org/10.47829/acmcr.2024.131602

Jeong, S. A., Yang, C., Song, J., Song, G., Jeong, W., & Lim, W. (2022). Hesperidin suppresses the proliferation of prostate cancer cells by inducing oxidative stress and disrupting Ca2+ homeostasis. Antioxidants (Basel), 11. https://doi.org/10.3390/antiox11091633

Kong, W., Ling, X., Chen, Y., Wu, X., Yao, W., Chen, X., & Zeng, Y. (2021). Hesperidin inhibits growth and angiogenesis of glioma. Frontiers in Pharmacology, 12, 733491. https://doi.org/10.3389/fphar.2021.733491

Kumar, S., Kumar, D., Sahu, M., & Kumar, A. (2020). Pharmacological and nanobiotechnological aspects of Gymnema Sylvestre. International Journal of Advanced Research (Indore), 8, 901–913. https://doi.org/10.21474/ijar01/11916

Lade, B. D., & Shanware, A. (2020). Phytonanofabrication: Methodology and factors affecting biosynthesis of nanoparticles. IntechOpen. https://doi.org/10.5772/intechopen.90918

Leau, S. A., Marin, Ş., Coară, G., Albu, L., Constantinescu, R. R., Kaya, M. A., & Neacşu, I. A. (2018). Study of wound-dressing materials based on collagen, sodium carboxymethylcellulose and silver nanoparticles used for their antibacterial activity in burn injuries. ICAMS Proceedings of the International Conference on Advanced Materials and Systems, 123–128. https://doi.org/10.24264/icams-2018.i.18

Liang, Z., Song, J., Xu, Y., Zhang, X., Zhang, Y., & Qian, H. (2022). Hesperidin reversed long-term N-methyl-N-nitro-N-nitroguanidine exposure induced EMT and cell proliferation by activating autophagy in gastric tissues of rats. Nutrients, 14. https://doi.org/10.3390/nu14245281

Nikolopoulou, S. G., Kalska, B., Basa, A., Papadopoulou, A., & Efthimiadou, E. K. (2023). Novel hybrid silver-silica nanoparticles synthesized by modifications of the sol-gel method and their theranostic potential in cancer. ACS Applied Bio Materials, 6, 5235–5251. https://doi.org/10.1021/acsabm.3c00494

Poomipark, N., Chaisin, T., & Kaulpiboon, J. (2023). Anti-proliferative, anti-migration, and anti-invasion activity of novel hesperidin glycosides in non-small cell lung cancer A549 cells. Research in Pharmaceutical Sciences, 18, 478. https://doi.org/10.4103/1735-5362.383704

Potara, M., Baia, M., Farcau, C., & Astilean, S. (2012). Chitosan-coated anisotropic silver nanoparticles as a SERS substrate for single-molecule detection. Nanotechnology, 23, 055501. https://doi.org/10.1088/0957-4484/23/5/055501

Rizvi, S. A. A., & Saleh, A. M. (2018). Applications of nanoparticle systems in drug delivery technology. Saudi Pharmaceutical Journal, 26, 64–70. https://doi.org/10.1016/j.jsps.2017.10.012

Rusdin, M., & Indonesian Journal of Pharmaceutics. (n.d.). Nanoparticles targeted drug delivery system via epidermal growth factor receptor: A review. Indonesian Journal of Pharmaceutics. Retrieved September 1, 2024, from https://jurnal.unpad.ac.id/idjp/article/view/23613

Tan, S., Dai, L., Tan, P., Liu, W., Mu, Y., Wang, J., Huang, X., & Hou, A. (2020). Hesperidin administration suppresses the proliferation of lung cancer cells by promoting apoptosis via targeting the MiR-132/ZEB2 signalling pathway. International Journal of Molecular Medicine, 46, 2069–2077. https://doi.org/10.3892/ijmm.2020.4756

TR, A., Selvaraju, K., & Gowrishankar, N. (2023). Biodegradable polymeric nanoparticles: The novel carrier for controlled release drug delivery system. International Journal of Science and Research Archive, 8, 630–637. https://doi.org/10.30574/ijsra.2023.8.1.0103

Wang, A. Z., Langer, R., & Farokhzad, O. C. (2012). Nanoparticle delivery of cancer drugs. Annual Review of Medicine, 63, 185–198. https://doi.org/10.1146/annurev-med-040210-162544

Wudtiwai, B., Makeudom, A., Krisanaprakornkit, S., Pothacharoen, P., & Kongtawelert, P. (2021). Anticancer activities of hesperidin via suppression of up-regulated programmed death-ligand 1 expression in oral cancer cells. Molecules, 26. https://doi.org/10.3390/molecules26175345

Yao, Y., Lin, M., Liu, Z., Liu, M., Zhang, S., & Zhang, Y. (2022). Hesperidin inhibits lung cancer in vitro and in vivo through PinX1. Frontiers in Pharmacology, 13, 918665. https://doi.org/10.3389/fphar.2022.918665

Zhao, J., Li, Y., Gao, J., & De, Y. (2017). Hesperidin inhibits ovarian cancer cell viability through endoplasmic reticulum stress signaling pathways. Oncology Letters, 14, 5569–5574. https://doi.org/10.3892/ol.2017.6873